



Targeted Inhibition of DNA-PKcs, ATM, ATR, PARP, and Rad51 Modulate Response to X Rays and Protons

Authors: Bright, Scott J., Flint, David B., Martinus, David K. J., Turner, Broderick X., Manandhar, Mandira, et al.

Source: Radiation Research, 198(4) : 336-346

Published By: Radiation Research Society

URL: <https://doi.org/10.1667/RADE-22-00040.1>

BioOne Complete (complete.BioOne.org) is a full-text database of 200 subscribed and open-access titles in the biological, ecological, and environmental sciences published by nonprofit societies, associations, museums, institutions, and presses.

Your use of this PDF, the BioOne Complete website, and all posted and associated content indicates your acceptance of BioOne's Terms of Use, available at www.bioone.org/terms-of-use.

Usage of BioOne Complete content is strictly limited to personal, educational, and non - commercial use. Commercial inquiries or rights and permissions requests should be directed to the individual publisher as copyright holder.

BioOne sees sustainable scholarly publishing as an inherently collaborative enterprise connecting authors, nonprofit publishers, academic institutions, research libraries, and research funders in the common goal of maximizing access to critical research.

Targeted Inhibition of DNA-PKcs, ATM, ATR, PARP, and Rad51 Modulate Response to X Rays and Protons

Scott J. Bright,^{a,1} David B. Flint,^{a,2} David K. J. Martinus,^{a,b,2} Broderick X. Turner,^{a,b,2} Mandira Manandhar,^{a,2} Mariam Ben Kacem,^{a,2} Conor H. McFadden,^{a,2,3} Timothy A. Yap,^c Simona F. Shaitelman,^{d,1} Gabriel O. Sawakuchi^{a,b,1}

^a Department of Radiation Physics, Division of Radiation Oncology, The University of Texas MD Anderson Cancer Center, Houston, Texas; ^b The University of Texas MD Anderson Cancer Center UTHealth Graduate School of Biomedical Sciences, Houston, Texas; ^c Department of Investigational Cancer Therapeutics (Phase I Clinical Trials Program), Division of Cancer Medicine; Khalifa Institute for Personalized Cancer Therapy; Department of Thoracic/Head and Neck Medical Oncology; and The Institute for Applied Cancer Science, The University of Texas MD Anderson Cancer Center, Houston, Texas; ^d Department of Radiation Oncology, Division of Radiation Oncology, The University of Texas MD Anderson Cancer Center, Houston, Texas

Bright SJ, Flint DB, Martinus DKJ, Turner BX, Manandhar M, Ben Kacem M, McFadden CH, Yap TA, Shaitelman SF, Sawakuchi GO. Targeted Inhibition of DNA-PKcs, ATM, ATR, PARP, and Rad51 Modulate Response to X Rays and Protons. *Radiat Res.* 198, 336–346 (2022).

Small molecule inhibitors are currently in preclinical and clinical development for the treatment of selected cancers, particularly those with existing genetic alterations in DNA repair and DNA damage response (DDR) pathways. Keen interest has also been expressed in combining such agents with other targeted antitumor strategies such as radiotherapy. Radiotherapy exerts its cytotoxic effects primarily through DNA damage–induced cell death; therefore, inhibiting DNA repair and the DDR should lead to additive and/or synergistic radiosensitizing effects. In this study we screened the response to X-ray or proton radiation in cell lines treated with DDR inhibitors (DDRi) targeting ATM, ATR, DNA-PKcs, Rad51, and PARP, with survival metrics established using clonogenic assays. We observed that DDRi generate significant radiosensitization in cancer and primary cells derived from normal tissue. Existing genetic defects in cancer cells appear to be an important consideration when determining the optimal inhibitor to use for synergistic combination with radiation. We also show that while greater radiosensitization can be achieved with protons (9.9 keV/μm) combined with DDRi, the relative biological effectiveness is unchanged or in some cases reduced. Our results indicate

that while targeting the DDR can significantly radiosensitize cancer cells to such combinations, normal cells may also be equally or more severely affected, depending on the DDRi used. These data highlight the importance of identifying genetic defects as predictive biomarkers of response for combination treatment. © 2022 by Radiation Research Society

INTRODUCTION

Poly (ADP-ribose) polymerase (PARP) inhibitors are approved for the treatment of a range of molecularly selected cancers (1–3). An ever-growing number of DNA damage response and repair (DDR) inhibitors (DDRi) are in development, with the hope they can be deployed to patients with tumors that have specific genetic alterations that render them exquisitely sensitive to a given DDRi (4). Keen interest has also been expressed in using these inhibitors to further sensitize tumors to radiation (5) since radiation treatment primarily acts through DNA damage-induced cell death (6, 7). Current radiation delivery techniques using image guidance allow precise targeting of radiation to the tumor while sparing nearby normal tissues. This provides a unique opportunity to combine radiation with systemic DDRi to preferentially radiosensitize the tumor and minimize toxicity to normal tissues (8, 9).

Clinically, the two major forms of radiation delivery include X rays (photons) and protons. These two forms of radiation vary based on their linear energy transfer (LET) and relative biological effectiveness (RBE), with protons having higher LET and RBE due to their ability to generate more clustered DNA lesions, often considered harder for cells to repair (10, 11). Protons also provide superior sparing of normal tissue and lower integral doses than X rays (12). Despite these physical differences, it remains uncertain what the biological implication is of combining distinct forms of radiation treatment with DDRi that target different stages and processes of DDR. Additionally,

¹ Corresponding authors: Scott J. Bright, PhD, Department of Radiation Physics, Division of Radiation Oncology, The University of Texas MD Anderson Cancer Center, 6565 MD Anderson Blvd, Houston, TX 77030-4008; email: sjbright@mdanderson.org. Simona F. Shaitelman, MD, EdM Department of Radiation Oncology, Division of Radiation Oncology, The University of Texas MD Anderson Cancer Center, 6565 MD Anderson Blvd, Houston, TX 77030-4008; email: SFShaitelman@mdanderson.org. Gabriel O. Sawakuchi, PhD, Department of Radiation Physics, Division of Radiation Oncology, The University of Texas MD Anderson Cancer Center, 6565 MD Anderson Blvd, Houston, TX 77030-4008; email: gsawakuchi@mdanderson.org.

² Scholar in Training.

³ Current address: The University of Texas Southwest Medical Center, 5323 Harry Hines Blvd, Dallas, TX 75390.

because DDRs can radiosensitize both normal and tumor tissues, interrogating the response of both tissue types to the combinations of radiation plus DDRs is an important part of enhancing the therapeutic ratio.

Cells have several pathways for responding to DNA lesions. The pathway of choice depends on the type of lesion, which may vary with LET and cell cycle stage (13–19). For DNA double-strand break (DSB) lesions, the DDR is activated through proteins that include ataxia-telangiectasia mutated (ATM) and ataxia telangiectasia and Rad3-related protein (ATR), which orchestrate repair and pause the cell cycle to allow time for proper resolution. Once sensed, DSB lesions are generally repaired via non-homologous end joining (NHEJ), which relies on DNA-dependent protein kinase, catalytic subunit (DNA-PKcs), or homologous recombination (HR), which relies on Rad51 (20). DNA-PKcs, ATM and ATR are key DDR proteins, members of the phosphoinositide 3-kinase-related kinases (PIKKs) family. Other DDR proteins include proteins such as poly ADP ribose polymerase (PARP), which is usually associated with repair of single-stranded lesions through base excision repair (BER) (21). Here we chose inhibitors that target proteins that are critical for DDR (ATM and ATR) because of their importance in orchestrating downstream processing of DNA lesions as well as proteins involved in specific DNA repair pathways including DNA-PKcs (NHEJ), Rad51 (HR) and PARP (BER). Our investigations focus on those DDRs which are already being investigated in clinical trials in combination with radiotherapy (Supplementary Table S1; <https://doi.org/10.1667/RADE-22-00040.1.S1>), namely, inhibitors of ATR, ATM, DNA-PKcs, and PARP. We also investigate an inhibitor of RAD51 that is not currently in clinical trials.

One major consideration in combining radiotherapy with DDRs is the potential for normal tissue toxicity. Radiotherapy combined with a PARP inhibitor led to an increase in skin and esophageal toxicity in a preclinical model (22). In addition, Jagsi et al. reported that 10% of patients receiving radiotherapy concurrent with a PARP inhibitor showed grade 3 toxicity one year after treatment and this increased to up to 50% after 3 years (23). Moreover, Loap et al. reported that at 1 year after treatment there was no grade 3 or greater toxicities although one patient did show a persistent grade 2 adverse event (24). Data on other inhibitors is relatively sparse. Here we demonstrate the effectiveness of a range of clinically-based DDRs combined with X rays or protons in lung and pancreatic cancer cell lines, in addition to a primary cell line derived from normal tissue to gauge potential therapeutic windows.

MATERIALS AND METHODS

Cell Lines and Cell Culture Conditions

Two lung cancer (NCI-H460 and NCI-H1299) and two pancreatic cancer (PANC-1 and Panc 10.05) cell lines were purchased from the American Type Culture Collection. NCI-H460 and NCI-H1299 cells

were cultured in RPMI-1640 (R8758, Sigma-Aldrich, St. Louis, MO) supplemented with 10% fetal bovine serum (FBS) (F0926, Sigma-Aldrich) and 1% penicillin-streptomycin (P/S) (SV30010, Hyclone, Cytiva, Marlborough, MA). PANC-1 and Panc 10.05 cells were cultured in DMEM (D6429, Sigma-Aldrich) supplemented with 10% FBS and 1% P/S. Cell lines were authenticated by using short tandem repeat markers and checked for mycoplasma contamination at the MD Anderson Cytogenetics and Cell Authentication Core facility before experiments. The human umbilical vein endothelial cell (HUVEC) line (kind gift from Dr. Keri Schadler, University of Texas MD Anderson Cancer Center) was used to understand potential effects in normal cells and identify DNA repair inhibitors that radiosensitize cancer cells more than normal cells. HUVECs are primary cells derived from normal tissue in 2D culture and are henceforth referred to as “normal cells.” HUVECs were cultured in endothelial cell medium (1001, ScienCell, Carlsbad, CA) supplemented with 5% FBS, 1% P/S, and 1% endothelial cell growth supplement. All cell lines were maintained in a humidified incubator with 5% CO₂ at 37°C. Other key resources are shown in Supplementary Table S2 (<https://doi.org/10.1667/RADE-22-00040.1.S2>). Cell lines were also analyzed for existing genetic defects in DNA repair genes [Supplementary Table S3 (<https://doi.org/10.1667/RADE-22-00040.1.S3>) and Supplementary Fig. S1 (<https://doi.org/10.1667/RADE-22-00040.1.S6>)] using the Cancer Cell Line Encyclopedia (CCLE) (26).

DNA Repair Inhibitors and Treatment

Inhibitors of DNA-PKcs (DNA-PKcsi) (NU7441, S2638, Selleck Chemicals LLC, Houston, TX), ATM (ATMi) (KU55933, S1092, Selleck Chemicals LLC), ATR (ATRi) (cerelastib, S7693, Selleck Chemicals LLC), PARP (PARPi) (AZD2281, olaparib, S1060, Selleck Chemicals LLC), and Rad51 (Rad51i) (B02, S8434, Selleck Chemicals LLC) were resuspended in dimethylsulfoxide (DMSO) (BP231, Fisher Scientific, Waltham, MA) at 10 mM except for NU7441, which was resuspended at 5 mM or purchased in DMSO at 10 mM. Resuspended inhibitors were stored at –80°C. Total incubation time with each inhibitor was 24 h (6–8 h before irradiation and 16–18 h postirradiation), after which media containing inhibitor was replaced with fresh media. A 6–8 h pre-incubation time was chosen to allow effective inhibition but also to allow reproducibility in experimental procedures for proton irradiations.

Irradiation Conditions

Cells were irradiated with either X rays or protons as described previously (25). Briefly, X rays were delivered by a 6-MV clinical linear accelerator (Truebeam, Varian Medical Systems, Palo Alto, CA) at a water equivalent depth of 10 cm with a dose rate of 4.4 Gy/min at the cells' position. X-ray irradiations were done in full scatter conditions, which was accomplished using a holder that could hold four 6-well plates. The plate holder minimized air gaps, provided enough lateral thickness for full lateral scatter and provided enough support to place additional plastic blocks above the plates for full backscatter. The plate holder with plates were placed above water equivalent plastic blocks, which were then placed on the treatment couch. We used 30 cm × 30 cm field size beams delivered at a 180° gantry angle at a source to surface distance of 100 cm to the bottom of the couch. The total water equivalence thickness from the bottom of the couch to the cells' position was 10 cm and the beam traversed the couch, water equivalent blocks, bottom of the plate holder and bottom of the 6-well plate before reaching the cells. To measure the X ray absorbed dose to water in a condition as close as possible to the condition to which we exposed the cells, we used gafchromic film cut out and placed in the wells of the 6-well plates under 3 mL of water to reproduce the thickness of the cell media. The 6-well plates were then placed in the plate holder in the same setup used for cell irradiations.

Protons were delivered at the MD Anderson Proton Therapy Center with an unmodulated 100-MeV proton beam at a water equivalent

depth of 4.42 cm, with a dose-weighted LET in water of 9.9 keV/μm. The LET was determined with a validated Monte Carlo model of the proton beam nozzle (26). Proton dose rate ranged from 1 to 3 Gy/min, depending on the stability of the beam for a given experiment. We used 18 cm × 18 cm field-size beams delivered at a 180° gantry angle at source-to-surface distance setup to the bottom of the couch. The beam crossed the couch, water-equivalent plastic blocks, and bottom of the 6-well plates to a combined water equivalent depth of 4.42 cm before reaching the cells. We typically exposed two 6-well plates at once. To measure the proton absorbed dose to water in a condition as close as possible to the condition to which we exposed the cells, we used a calibrated parallel plate ionization chamber (34045, Advanced Markus Chamber, PTW-Freiburg, Freiburg, Germany) with cutouts of the bottom of the 6-well plates to reproduce the water equivalent thickness of the experimental setup used for the cell irradiations.

Clonogenic Cell Survival

Clonogenic assays were performed as described previously (25, 27). Briefly, cells were seeded into 6-well plates at various numbers, depending on the dose to be delivered. Cell numbers were optimized for each cell line to obtain 20–60 colonies per well. After irradiation, cell lines were left in the incubator to form colonies for 7–21 days, after which colonies were stained with 2% crystal violet (HT90132, Sigma-Aldrich) in 100% ethanol. Plates were then scanned using a high-resolution flatbed scanner (Expression 10000 XL, Epson, Long Beach, CA). Images were analyzed using an ImageJ plugin optimized for each cell line to count colonies containing 50 or more cells, as previously described (25). For each cell line, brightness and cell density thresholds were established to exclude noise. We calculated the minimum area for colonies containing 50 cells and segmented colonies that exceeded this threshold. At least three biological repeats were performed for each condition. Each biological repeat contained at least two replicates.

Data and Statistical Analyses

Data were analyzed as previously described (25, 27). Briefly, data were fit to the linear quadratic model, in which the survival fraction $SF = \exp(-\alpha D - \beta D^2)$ expression was used to extract the survival fraction at 2 Gy (SF_{2Gy}), the doses at 50% ($D_{50\%}$) and 10% ($D_{10\%}$) survival fractions, and the mean inactivation dose (MID). The MID was calculated as described previously (28–31). Briefly, for each condition the survival curve was numerically integrated from dose 0 to infinity using MATLAB (R2022a, MathWorks, Natick, MA).

Values for α and β are included in Supplementary Table 4 (<https://doi.org/10.1667/RADE-22-00040.1.S4>) and derived sensitivity metrics are included in Supplementary Table 5 (<https://doi.org/10.1667/RADE-22-00040.1.S5>). The following metrics were derived for comparisons between radiation types, treatment with inhibitors, and combinations of radiation and inhibitors:

$$SER_{r,i}(M) = \frac{M_{r,DMSO}}{M_{r,i}}, \quad (1)$$

$$RBE_i(M) = \frac{M_{X\ ray,i}}{M_{proton,i}}, \quad (2)$$

$$TSE_{r,i}(M) = \frac{M_{X\ ray,DMSO}}{M_{r,i}}, \quad (3)$$

where M is the parameter in question [SF_{2Gy} , $D_{50\%}$, $D_{10\%}$, or MID], i is the inhibitor, and r is radiation type. The sensitization enhancement ratio (SER) was used to quantify the effect of an inhibitor with a given type of radiation. The RBE was used to quantify the effect of LET when a certain inhibitor was used. Finally, the total sensitivity enhancement (TSE) was used to quantify the total gain in

radiosensitivity, comparing both types of radiation and inhibitor combinations to X rays with DMSO (for X rays, the TSE is equivalent to the SER).

Data were analyzed with GraphPad Prism version 7.03 for Windows. Unpaired t tests were used to compare differences between survival metrics. The sample size of parameters calculated from ratios of two variables with different sample sizes (e.g., SER, RBE or TSE) was set to the sample size of the variable with the lower number of samples.

RESULTS

We examined HUVEC cells and the four cancer cell lines. The existing genetic defects in the DNA repair and DDR genes for these cancer cell lines are shown in Supplementary Table S3 (<https://doi.org/10.1667/RADE-22-00040.1.S3>) and Supplementary Fig. S1 (<https://doi.org/10.1667/RADE-22-00040.1.S6>). Panc 10.05 generally showed deletions in several genes, while NCI-H1299 showed many amplifications, including the NHEJ gene PRKDC (DNA-PKcs). NCI-H460, which is TP53 wild-type, showed the fewest alterations, while the other cell lines either showed deep deletions (NCI-H1299 and Panc 10.05) or missense mutations (PANC-1) in TP53. All cell lines showed different inherent radiosensitivities to X rays and protons, with significantly lower SF_{2Gy} for protons (Fig. 1). NCI-H460 was the most radiosensitive, whereas NCI-H1299 was the most radioresistant cell line tested. The same trends were observed for the MID, $D_{50\%}$ and $D_{10\%}$ [Supplementary Fig. S3 (<https://doi.org/10.1667/RADE-22-00040.1.S6>) and Supplementary Table S5 (<https://doi.org/10.1667/RADE-22-00040.1.S5>)].

Each inhibitor alone showed minimal effects on plating efficiency (Supplementary Fig. S2; <https://doi.org/10.1667/RADE-22-00040.1.S6>), except for HUVEC and Panc 10.05 cells treated with 2 μM ATR, which showed plating efficiencies ranging from ~55–60%. In most cases, combining DNA-PKcsi, ATMi, or ATRi (PIKKs inhibitors) with protons was more effective than combining them with X rays (Fig. 2A–O); this was also the case for MID, $D_{50\%}$ and $D_{10\%}$ (Supplementary Figs. S4 and S5; <https://doi.org/10.1667/RADE-22-00040.1.S6>). Exceptions included NCI-H1299, which had a significantly lower SF_{2Gy} for X rays than for protons when treated with 0.1 μM ATRi, 0.1 μM ATMi and 0.5 μM DNA-PKcsi (Fig. 2C, 2H, 2M). HUVEC and PANC-1 had significantly lower SF_{2Gy} with protons for all three PIKKs inhibitors tested (Fig. 2A, 2D, 2F, 2I, 2K, 2N). NCI-H460 and NCI-H1299 showed very poor colony formation after exposure to 2 μM ATRi (Supplementary Fig. S2; <https://doi.org/10.1667/RADE-22-00040.1.S6>) and therefore this condition was not assessed with either radiation type for these cell lines.

Protons were significantly more effective at reducing SF_{2Gy} , MID, $D_{50\%}$, and $D_{10\%}$ with either PARPi or Rad51i than were X rays with the same inhibitor for cancer and HUVEC cell lines, with the one exception of the NCI-H1299 cell line with Rad51i, which showed no difference

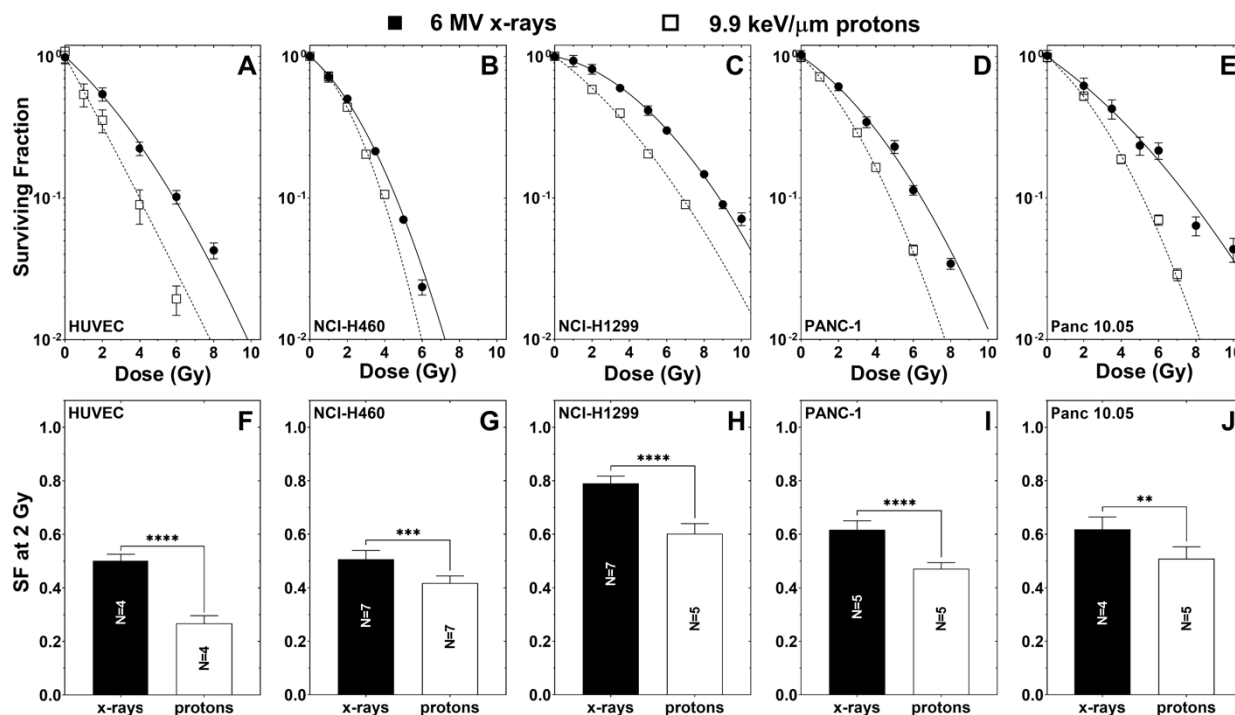


FIG. 1. Survival curves (panels A–E) and SF_{2Gy} (panels F–J). Error bars represent the standard deviation. Lines represent a fit using the linear quadratic model. N represents the number of biological replicates. * $P < 0.05$; ** $P < 0.01$; *** $P < 0.001$; and **** $P < 0.0001$.

between protons and X rays [Fig. 3; Supplementary Figs. S6 and S7 (<https://doi.org/10.1667/RADE-22-00040.1.S6>); Supplementary Table S5 (<https://doi.org/10.1667/RADE-22-00040.1.S5>)].

DNA-PKcsi increased SER_{SF2Gy} , SER_{MID} , $SER_{D50\%}$ and $SER_{D10\%}$ to protons and X rays, an effect that was universally seen at higher (0.5 μM) concentrations (Fig. 4A–E, and Supplementary Table S5; <https://doi.org/10.1667/RADE-22-00040.1.S5>).

ATMi significantly radiosensitized NCI-H460 to protons and NCI-H1299 to X rays. The SER_{SF2Gy} values were smaller than unity for the NCI-H1299 and Panc 10.05 cell lines exposed to protons + ATMi (Fig. 4A–E). These effects were also apparent at MID and $D_{50\%}$ but not at $D_{10\%}$ (Supplementary Table 5; <https://doi.org/10.1667/RADE-22-00040.1.S5>).

ATRi significantly radiosensitized cells to both X rays and protons, although PANC-1 showed no significant radiosensitization at a lower concentration (0.1 μM) but did at a higher concentration (2 μM) (Fig. 4A–E, and Supplementary Table S5; <https://doi.org/10.1667/RADE-22-00040.1.S5>). Panc 10.05 showed no significant radiosensitization at 0.1 μM ATRi for either X rays or protons but was radiosensitized with 2 μM ATRi.

PARPi significantly radiosensitized HUVECs, NCI-H460, NCI-H1299, and PANC-1 (Fig. 4A–E, and Supplementary Table S5; <https://doi.org/10.1667/RADE-22-00040.1.S5>). The greatest effect was seen in NCI-H460 cells exposed to protons. Very little difference was observed in radiosensitization between radiation type for PARPi.

PARPi did not significantly radiosensitize Panc 10.05 to X rays or protons, although sensitization did increase for Panc 10.05 when MID, $D_{50\%}$ and $D_{10\%}$ were compared (Supplementary Table S5; <https://doi.org/10.1667/RADE-22-00040.1.S5>).

Finally, Rad51i led to very little radiosensitization (Fig. 4A–E, and Supplementary Table S5; <https://doi.org/10.1667/RADE-22-00040.1.S5>). NCI-H460 cells exposed to X rays and treated with Rad51i showed significantly reduced SER_{SF2Gy} . Very few differences were noted at $D_{50\%}$, but NCI-H460 and Panc 10.05 increased sensitivity for MID and $D_{10\%}$ (Supplementary Table S5; <https://doi.org/10.1667/RADE-22-00040.1.S5>).

To analyze the gain in radiosensitization in cancer cells relative to normal HUVECs, we calculated the ratios of SER_{SF2Gy} for cancer cells compared to normal HUVECs. Values below unity indicate normal cells were, relatively radiosensitized more than cancer cells. For most scenarios of protons or X rays with DDRi, the investigated cancer cell lines were equally or more radiosensitized than the HUVEC (Fig. 5A–D).

HUVECs generally showed a higher RBE_{SF2Gy} relative to cancer cells for all DDRis (Fig. 6A–E). The RBE_{SF2Gy} for all inhibitors was variable by concentration and cell line. The RBE_{SF2Gy} of NCI-H460 was increased after treatment with most of the DDRis, but the RBE_{SF2Gy} of NCI-H1299 was decreased for most of the DDRis. In general, protons combined with DDRis were more effective in cell killing than X rays combined with the respective DDRi (Fig. 6F–J). However, we observed that DNA-PKcsi at 0.5 μM and

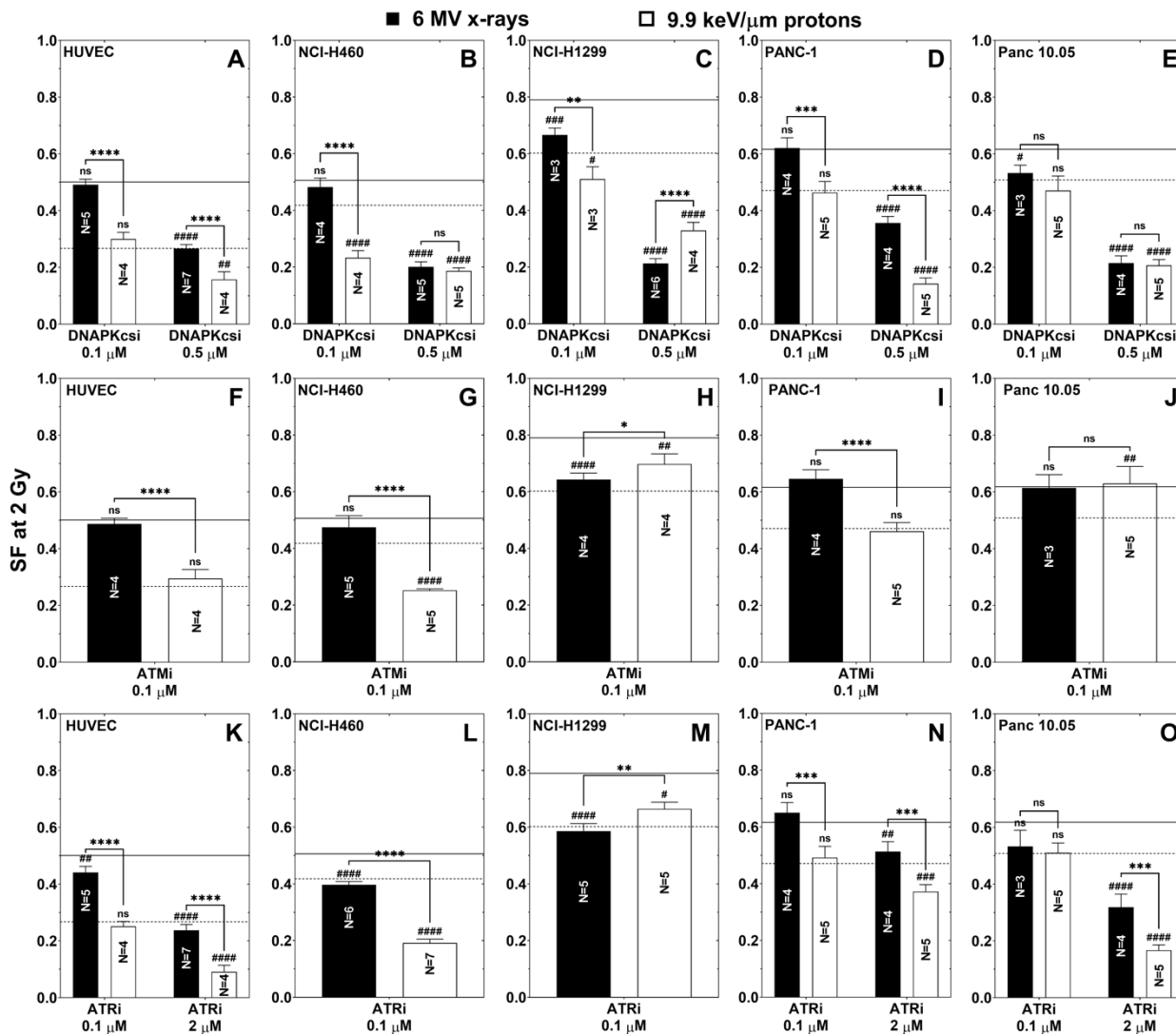


FIG. 2. SF_{2Gy} for combinations of DDRis with X rays or protons: (panels A–E) RT+DNA PKcsi; (panels F–J) RT + ATMi; and (panels K–O) RT + ATRi. Lines represent responses to X rays (solid) and protons (dashed) when treated with DMSO alone, without DDRi. Significance denotes differences between X rays and protons with a given inhibitor (*) or differences between a given inhibitor/radiation pair and its respective radiation type with DMSO (respective line) (#). Error bars represent the standard deviation. N represents the number of biological replicates. ns: not significant; * or # $P < 0.05$; ** or ## $P < 0.01$; *** or ### $P < 0.001$; and **** or #### $P < 0.0001$.

ATRi at 0.1 μM generated higher cell kill for X rays than protons for the NCI-H1299 cell line.

DISCUSSION

Using a variety of DDRis, we have demonstrated radiosensitization to both X rays and protons in several cancer cell lines and in a primary endothelial cell derived from normal tissue. Our results demonstrate that significant radiosensitization can be achieved with DDRis, particularly those targeting DNA-PKcs, ATM, ATR, PARP, or Rad51. Notably, in some cases the normal cell line evaluated was equally or more radiosensitized compared with cancer cell lines. We further demonstrated that generally, greater radiosensitization was achieved with protons, but this did not translate to greater RBE; in some cases, RBE was

significantly reduced. This raises important questions as to the relevance of RBE in the context of different LET values when radiotherapy is combined with radiosensitizers. It appears that DDRis can both increase and reduce RBE compared to the baseline with no DDRi, therefore several factors would need to be considered when prescribing dose, including the direction in which RBE might move and the RBE in normal tissue. We also showed that the efficacy of a DDRi depends strongly on a combination of factors, including the cell line, targeted DDR protein, and type of radiation. Some combinations generated profound radiosensitization and others very modest or no radiosensitization. This indicates the importance of identifying biomarkers that can predict the efficacy of a DDRi combined with a specific type of radiation before application in the clinic, such as pre-existing DNA repair defects. Further studies investigat-

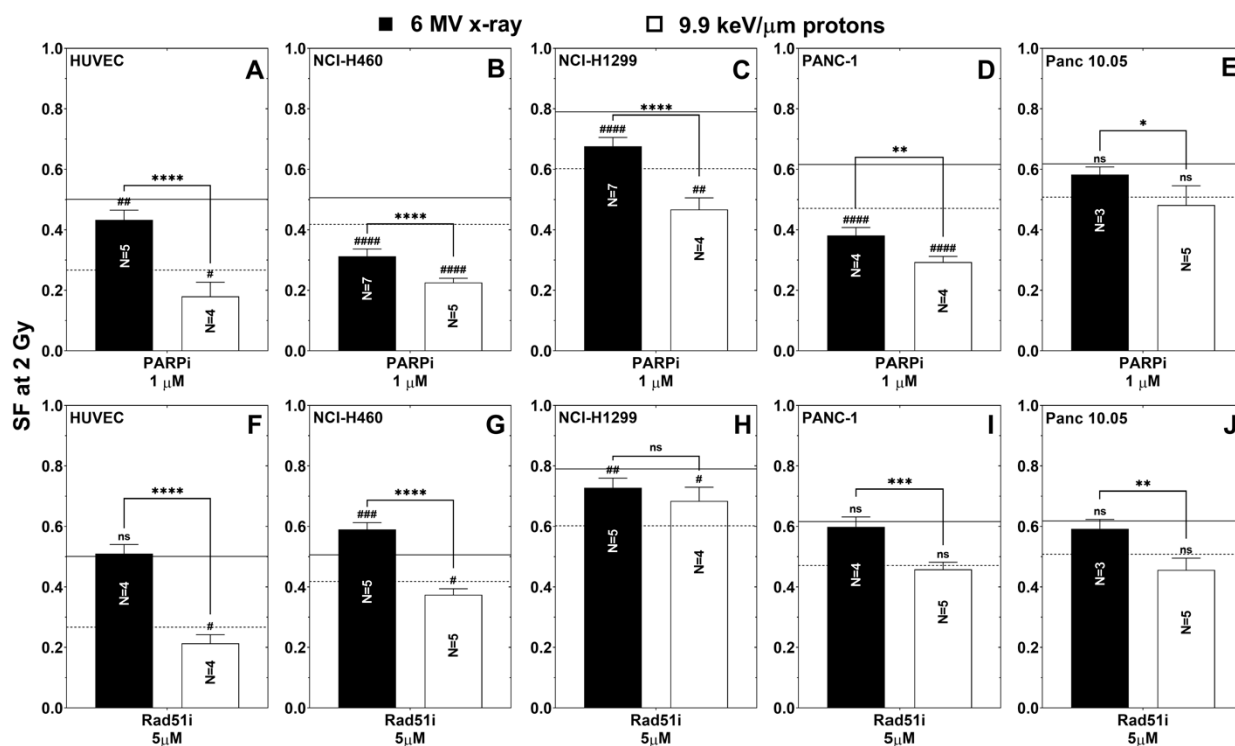


FIG. 3. SF_{2Gy} for combinations of DDRIs with X rays or protons: Panels A–D: RT + PARPi; and panels F–J: RT + Rad51i. Lines represent responses to X rays (solid) and protons (dashed) when treated with DMSO alone, without DDRi. Significance denotes differences between X rays and protons with a given inhibitor (*) or differences between a given inhibitor/radiation pair and its respective radiation type with DMSO (respective line) (*). Error bars represent the standard deviation. N represents the number of biological replicates. ns: not significant; * or #P < 0.05; ** or ##P < 0.01; *** or ###P < 0.001; and **** or ####P < 0.0001.

ing other genetic backgrounds with more genetic defects in DNA repair and DDR genes are warranted and may reveal unique combinations that may synergize with X rays or protons to radiosensitize.

Understanding the radiosensitizing effects of DDRi on tumor cells relative to normal cells is essential given that radiotherapy doses are often constrained by normal tissue toxicity. Despite the gains in radiosensitivity for cancer cell

lines, HUVECs were in some cases radiosensitized more than cancer cells. HUVECs are endothelial cells, a model that is relevant for tumor vascularization. Endothelial cell death may promote tumor radiosensitization as a previous study showed that microvascular endothelial cell death can significantly disrupt tumor growth following radiation (32). We believe the sensitivity of HUVECs is due to their ability to recognize unrepaired lesions and initiate cell death

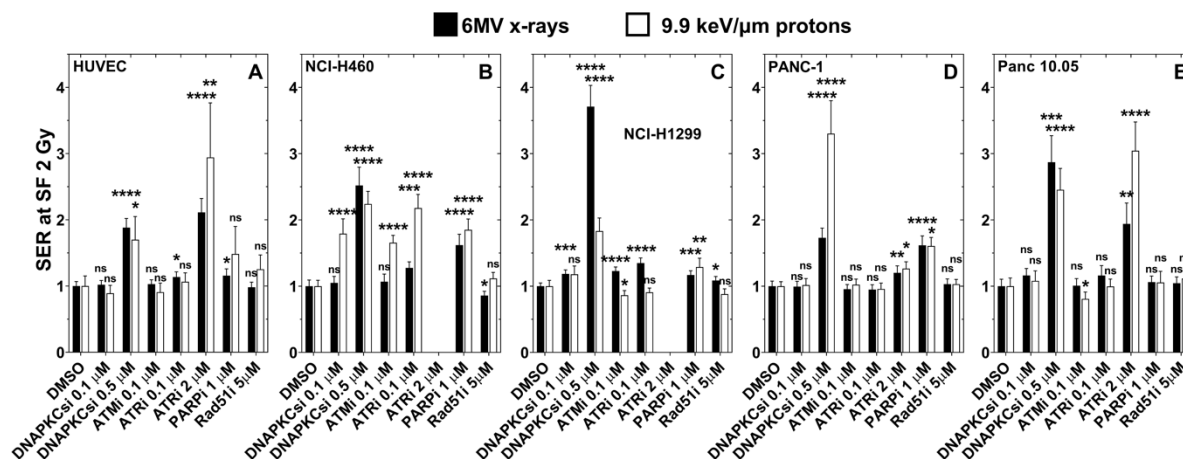


FIG. 4. Panels A–E: SER_{SF2Gy} for combinations of DDRIs with X rays or protons. Significance denotes differences between combinations of radiation/DDRi and the respective radiation alone (DMSO). Sample sizes used for the statistical analyses are presented in Figs. 1–3. Error bars represent the standard deviation. ns: not significant; *P < 0.05; **P < 0.01; ***P < 0.001; and ****P < 0.0001.

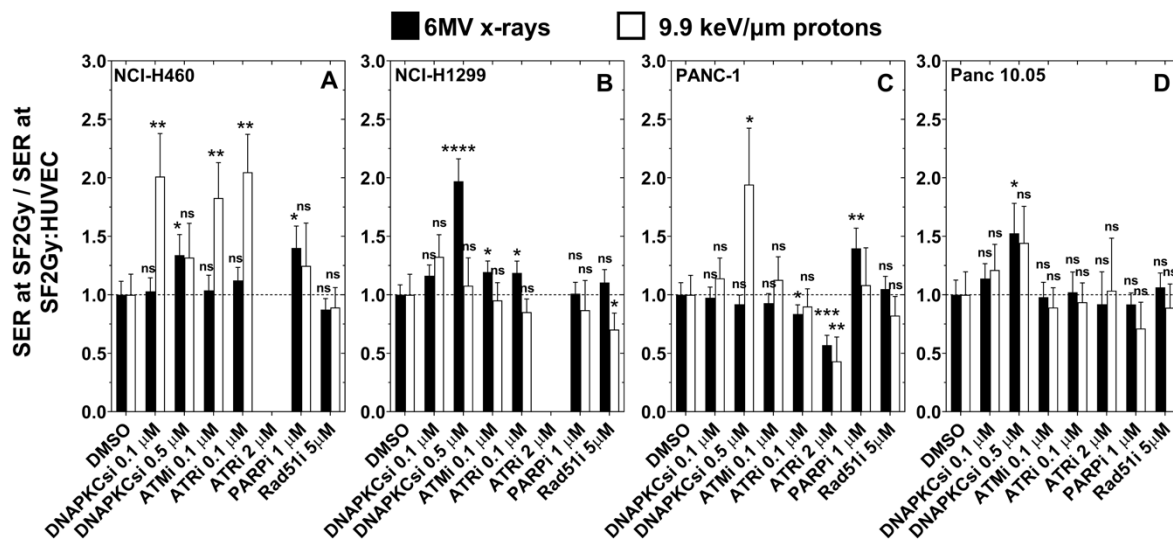


FIG. 5. Panels A–D: SER_{SF2Gy} of cancer cell lines relative to the SER_{SF2Gy} of HUVECs. Values below unity (dashed lines) indicate that the HUVEC (normal cell line) is radiosensitized relatively more than the respective cancer cell line. Significance denotes differences between combinations of radiation/DDRi and the respective radiation alone (DMSO). Sample sizes used for the statistical analyses are presented in Figs. 1–3. Error bars represent the standard deviation. ns: not significant; * $P < 0.05$; ** $P < 0.01$; *** $P < 0.001$; and **** $P < 0.0001$.

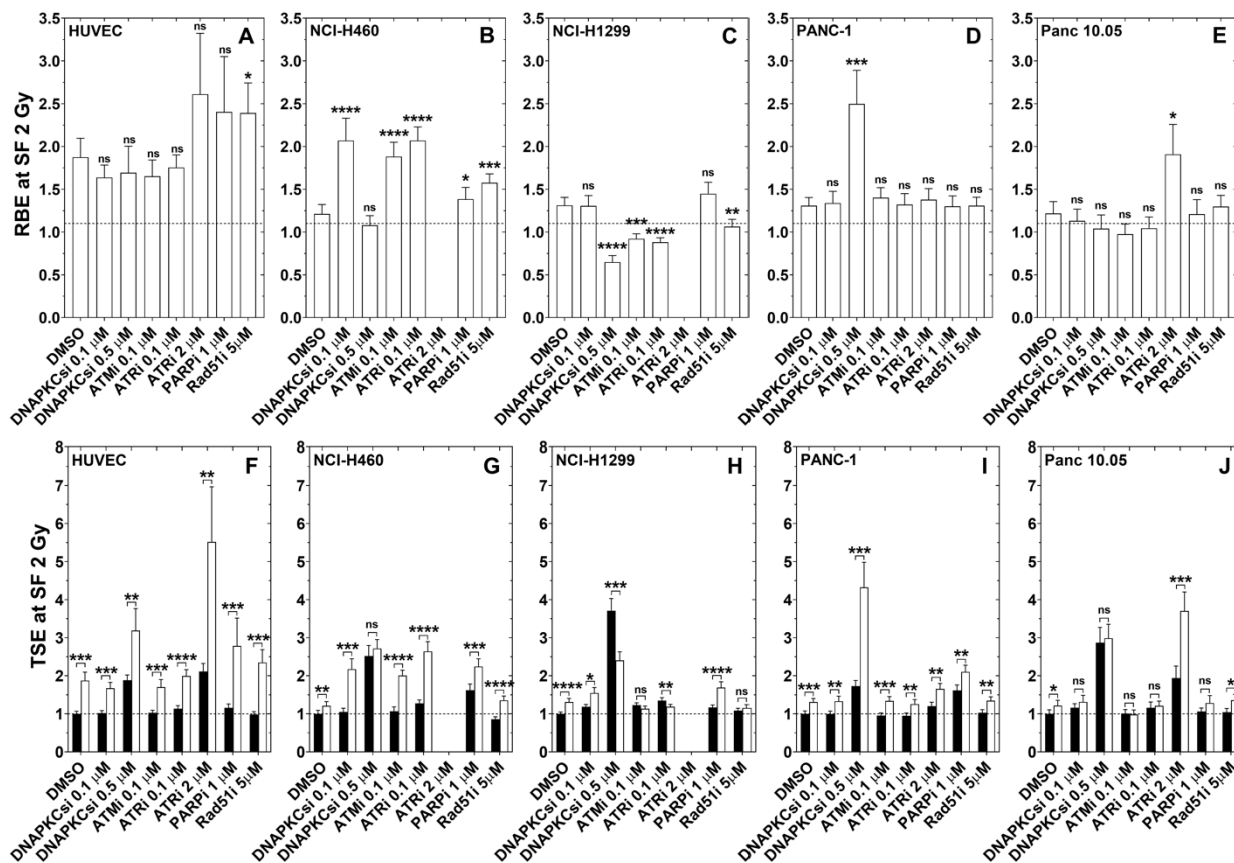


FIG. 6. Panels A–E: RBE_{SF2Gy} for the combination of DDRis with X rays or protons. Dashed lines refer to a $RBE_{SF2Gy} = 1.1$. Panels F–J: TSE_{SF2Gy} for combinations of DDRis with X rays or protons. Note that the TSE for X ray is equivalent to the SER. Dashed lines refer to TSE for X rays with DMSO. Panels A–E: Significance denotes differences between RBE_{SF2Gy} with DDRi and RBE_{SF2Gy} with DMSO. Panels F–J: Significance denotes differences between X rays and protons for a given DDRi. Sample sizes used for the statistical analyses are presented in Figs. 1–3. ns: not significant; * $P < 0.05$; ** $P < 0.01$; *** $P < 0.001$; and **** $P < 0.0001$.

processes to prevent further growth. In contrast, compensatory repair mechanisms within cancer cells, particularly those that accommodate DNA replication and bypass DNA damage lesions and the lack of cell cycle regulation both prevent cancer cells from initiating cell death after radiation injury. Without a predisposing alteration, cancer cells may be relatively less or comparably responsive to radiation + DDRi than normal cells that have intact machinery to sense DNA damage, regulate cell cycle, and activate cell death pathways. These alterations could then serve as a biomarker for selection of combinatorial treatments. It is also worth noting that effects of radiation combined with DDRi may be different in normal epithelial cells – particularly those with a high turnover rate, such as cells from the gastrointestinal tract. Because of the already increased cell cycle rate, DDRi that abrogate cell cycle checkpoints, such as ATRi and ATMi, may be more effective in radiosensitizing than other DDRi. It is possible that cells with a high turnover rate may be in G2 more frequently and therefore rely more on HR. Indeed, we observed that Rad51i led to increased radiosensitization in HUVECs.

We observed that inhibiting DNA-PKcs was extremely effective at radiosensitizing all cell types tested. Others have also observed radiosensitization through DNA-PKcs inhibition both in vivo and in vitro (33–36). Radiosensitization has also been observed with high-LET carbon-ion radiation treatment with the DNA-PKcs inhibitor NU7441. Sunada et al. (36) observed radiosensitization with NU7441 and attributed it to G2/M cell cycle arrest rather than DNA damage repair. Sunada et al. (36) also used NCI-H1299 cells but observed a much lower SER for X rays than observed here. Other inhibitors of DNA-PKcs such as AZD7648 (37), M3814 (38), and NU5455 (39) have shown similar radiosensitizing effects compared to the data presented here with NU7441. In these previous studies, radiosensitization was generally attributed to reduced NHEJ capacity. In our studies, DNA-PKcs at 0.5 μ M was the only treatment that significantly radiosensitized all the cell lines examined to both X rays and protons, with a consistent gain in radiosensitization for cancer cell lines over HUVECs. However, the RBE was decreased for NCI-H1299 cells. Also, in NCI-H1299, protons seemed to provide a lower TSE than did X rays (Fig. 6H), indicating that not all combinations of DDRi with protons will be superior to those with X rays. Nevertheless, the DNA-PKcs inhibitor did radiosensitize cells to both X rays and protons. We suggest that because of the importance of DNA-PKcs in NHEJ and the fact NHEJ is critical for timely repair of DSB lesions, inhibiting DNA-PKcs offers greater radiosensitization than other inhibitors.

ATM is considered a master regulator of cellular response to radiation-induced DNA damage (40), and as such is an attractive target for radiosensitization. Mutations in ATM have been shown to lead to radiosensitivity both in cancer (41) and in normal tissue, even with heterozygous somatic mutations (42). ATM inhibition has shown radiosensitizing effects in vitro and in vivo (43–46). Our results showed that

the ATM inhibitor KU55933 at 0.1 μ M had no effects on the response of HUVECs to radiation. NCI-H1299 and Panc 10.05 both showed elevated SF_{2Gy} with ATMi, although this was only observed for protons. This suggests ATM disruption under these specific circumstances modestly prevents cell death. We hypothesize that at this dose of inhibitor and survival endpoint, incomplete inhibition of ATM could lead to accumulation of more non-lethal DNA damage that activates compensatory repair mechanisms or transcription of more DNA repair factors. For example, ATM and ATR work in parallel or redundant pathways to abrogate cell cycle checkpoints (47). These survival patterns were not observed at D_{10%}, which may be because at higher doses (5–8 Gy in this case), radiation itself produces sufficient damage to overwhelm repair, which makes cell death less dependent on the DNA repair status.

ATR has also been an attractive target for its role in DNA repair and the cell cycle (48, 49). ATR inhibitors have shown promising radiosensitization in several models (50, 51). Radiosensitization seems to be driven by residual DNA damage and cell cycle checkpoint abrogation. In addition to radiosensitization, ATR inhibition combined with radiation has been shown to augment immune activation (52, 53) and promote antitumor activity. We saw significant radiosensitization with the ATR inhibitor ceralasertib to both X rays and protons. Because of ATR's role in HR and processing replication stress, we hypothesized that ATR may be more relevant for high-LET-induced clustered DNA damage because of the increased dependence on HR and additional time required to repair those lesions (10, 25, 54–57). However, only NCI-H460 showed significant increases in RBE. Nevertheless, HR relevance increases with LET; for the range of LET found in clinical proton beams, NHEJ is still by far the main DSB repair pathway (25). Thus, the LET of protons may not be high enough for synergy with ATR inhibition, and a higher LET associated with carbon-ion irradiation may be needed.

We found PARP inhibition radiosensitized all cell lines except Panc 10.05. Others have also reported radiosensitization by PARP inhibition (58–61). PARP1 is chiefly associated with the repair of single-strand breaks (62), but was also implicated recently in non-canonical DSB repair pathways (63, 64). When PARP inhibitors bind to PARP, a large proportion of their cytotoxic effects are thought to be derived from PARP trapping, in which PARP is still recruited to the lesion but the inhibitor prevents its dissociation from the lesion, resulting in failed repair, replication fork collapse, and DNA DSBs (65). Our results demonstrate radiosensitization in both lung and pancreatic cancer models, which in some cases exceeded 1.5-fold. Furthermore, we showed that PARP inhibition combined with protons significantly increased RBE in NCI-H460 cells. Additional investigations are required to confirm the proportion of increased radiosensitivity attributable to inhibiting PARP vs PARP trapping (66).

Rad51 is crucial for successful DNA repair via HR. Small molecule inhibitors of Rad51 have shown modest radiosensitization (67). Silencing Rad51 has also demonstrated radiosensitization (68). Several groups have shown that as LET increases, the relative importance of HR increases relative to NHEJ (25, 54, 69), and thus Rad51 inhibition has the potential to synergize with protons. However, our findings of only modest radiosensitization effects agree with those of Ma et al. (67). Significant increases in RBE were noted in HUVECs and NCI-H460 cells, both of which are TP53 wild-type. These observations that only modest radiosensitization could be achieved by inhibiting Rad51 could be explained by incomplete inhibition of Rad51 at this concentration.

Significant increases in RBE were only observed in a few conditions and did not appear consistent for a given inhibitor, highlighting the need for biomarkers to select appropriate combinations. Cells with existing genetic alterations may be hypersensitive to the combination of a specific DDRi and proton treatment.

Although we used the “gold-standard” clonogenic survival assay to assess radiation response when various DDR proteins were inhibited, we acknowledge that these assays fail to recreate many important microenvironmental cues such as hypoxia, amongst others. The inhibitors were also assessed under specific incubation conditions including a 24-h incubation time with an administration 6–8 h prior to irradiation. Scheduling could also be an important factor in determining response, particularly total incubation time. This work is limited to data on clonogenic cell survival only to characterize the response of several cell lines to several DDRis and it did not attempt to understand the mechanisms of each DDRi. Future work should be focused on elucidating the mechanisms of each DDRi on radiation response, with the goal of identifying biomarkers that could be used to select patients who will be responsive to the combination of a particular DDRi with a particular type of therapeutic radiation (photons, protons, carbon ions). We also believe further investigation is required in preclinical and clinical models to understand the immunomodulatory effects of DDRis combined with X rays or protons and the combinations’ ability to stimulate production of cytoplasmic DNA and downstream interferon signaling or immunogenic forms of cell death.

Our findings further indicate that, in some cases (Rad51 and ATR inhibitors), the HUVEC normal cell line seems to be radiosensitized more by DDRis than the cancer cell lines we tested here, which may have been because these cells are proliferating and dividing. More comprehensive studies of the extent of radiosensitization of normal cells by DDRis will require testing other normal cell lines as well as spheroid and in vivo models, particularly those that are not under proliferative pressure. In this case, senescence may become an important endpoint to consider.

Current radiotherapy technologies using beam modulation, sophisticated image guidance and motion management allow radiation to be delivered safely, with very high-dose gradients to target the tumor volume while sparing nearby

critical structures. Thus, by design, current radiation treatment plans are optimized to constrain the exposure of nearby critical structures to low doses of radiation. In this scenario, even if a DDRi radiosensitizes normal tissue more than tumor cells, a combination of a DDRi and radiation may still increase relative tumor cell kill. This may be even more apparent with proton radiotherapy, for which, in addition to dose gradients, there are LET gradients that may maximize tumor tissue effects and reduce normal tissue effects, all of which warrants further study.

CONCLUSIONS

DDRis can offer significant radiosensitization in the models tested here. Radiosensitization was inconsistent across cell lines and DDRis, which reinforces the need for biomarkers to guide combination treatment approaches. We also noted that DNA-PKcsi seemed to be the most effective radiosensitizer, highlighting the importance of NHEJ in radiation response. Further work is needed to identify DDRis that pair best with different radiation modalities, whilst minimizing effects on normal tissue and, more importantly, to find biomarkers that can predict the effect of a specific DDRi when combined with a specific type of radiation.

ACKNOWLEDGMENTS

This work was supported in part by funds from: the Cancer Prevention and Research Institute of Texas grant RP170040 (GOS); the University Cancer Foundation via the Sister Institution Network Fund at The University of Texas MD Anderson Cancer Center (GOS); The University of Texas MD Anderson Cancer Center Institutional Research Grant (IRG) program (GOS and SFS); the Department of Radiation Physics (Department chair funds from Dr. Mary K. Martel), The University of Texas MD Anderson Cancer Center; the Cancer Center Support (Core) Grant CA016672 to The University of Texas MD Anderson; R21CA252411 (SFS and GOS); NIH P01CA261669 (SFS and GOS); and Emerson Collective Foundation (SFS). The authors thank Christine F. Wogan, Division of Radiation Oncology at MD Anderson, for editing the manuscript. GOS and SFS have received research funds from TAE Life Sciences, Alpha Tau Medical and Artios Pharma. SFS has a research agreement with Exact Sciences. TAY Employment: Medical Director of the Institute for Applied Cancer Science (IACS), which has a commercial interest in DDR and other inhibitors. Research support (to institution): Artios, AstraZeneca, Bayer, Clovis, Constellation, Cyteir, Eli Lilly, EMD Serono, Forbius, F-Star, GlaxoSmithKline, Genentech, ImmuneSensor, Ipsen, Jounce, Karyopharm, Kyowa, Merck, Novartis, Pfizer, Ribon Therapeutics, Regeneron, Repare, Sanofi, Scholar Rock, SeaGen, Tesaro, and Vertex. Consultancy or advisory role: Almac, Aduro, AstraZeneca, Atrin, Axiom, Bayer, Bristol Myers Squibb, Calithera, Clovis, Cybrea, EMD Serono, F-Star, Guidepoint, Ignyta, I-Mab, Jansen, Merck, Pfizer, Repare, Roche, Rubius, Schrodinger, Seagen, Varian, and Zai Lab.

Received: February 5, 2021; accepted: July 5, 2022; published online: August 8, 2022

REFERENCES

1. Farmer H, McCabe N, Lord CJ, Tutt AN, Johnson DA, Richardson TB, et al. Targeting the DNA repair defect in BRCA mutant cells as a therapeutic strategy. *Nature* 2005; 434:917-21.
2. Bryant HE, Schultz N, Thomas HD, Parker KM, Flower D, Lopez

- E, et al. Specific killing of BRCA2-deficient tumours with inhibitors of poly(ADP-ribose) polymerase. *Nature* 2005; 434:913-7.
3. Faraoni I, Graziani G, Role of BRCA mutations in cancer treatment with Poly(ADP-ribose) polymerase (PARP) inhibitors. *Cancers (Basel)* 2018; 10:487.
 4. Cleary JM, Aguirre AJ, Shapiro GI, D'Andrea AD, Biomarker-guided development of DNA repair inhibitors. *Mol Cell* 2020; 78:1070-85.
 5. Morgan MA, Lawrence TS, Molecular pathways: Overcoming radiation resistance by targeting DNA damage response pathways. *Clin Cancer Res* 2015; 21:2898-904.
 6. Surova O, Zhivotovsky B, Various modes of cell death induced by DNA damage. *Oncogene* 2013; 32:3789-97.
 7. Roos WP, Kaina B, DNA damage-induced cell death: from specific DNA lesions to the DNA damage response and apoptosis. *Cancer Lett* 2013; 332:237-48.
 8. Lloyd RL, Wijnhoven PWG, Ramos-Montoya A, Wilson Z, Illuzzi G, Falenta K, et al. Combined PARP and ATR inhibition potentiates genome instability and cell death in ATM-deficient cancer cells. *Oncogene* 2020; 39:4869-83.
 9. Lin SH, Willers H, Krishnan S, Sarkaria JN, Baumann M, Lawrence TS, Moving Beyond the Standard of Care: Accelerate Testing of Radiation-Drug Combinations. *Int J Radiat Oncol Biol Phys*. 2021; 111:1131-39.
 10. Nickoloff JA, Sharma N, Taylor L, Clustered DNA double-strand breaks: biological effects and relevance to cancer radiotherapy. *Genes (Basel)* 2020; 11.
 11. Paganetti H, Relative biological effectiveness (RBE) values for proton beam therapy. Variations as a function of biological endpoint, dose, and linear energy transfer. *Phys Med Biol* 2014; 59, R419-72.
 12. Paganetti H, Beltran C, Both S, Dong L, Flanz J, Furutani K, et al. Roadmap: proton therapy physics and biology. *Phys Med Biol* 2021; 66:05RM01.
 13. Iliakis G, Mladenova V, Sharif M, Chaudhary S, Mavragani IV, Soni A, et al. Defined biological models of high-LET radiation lesions. *Radiat Prot Dos* 2018; 183:60-68.
 14. Fontana AO, Augsburg MA, Grosse N, Guckenberger M, Lomax AJ, Sartori AA, et al. Differential DNA repair pathway choice in cancer cells after proton- and photon-irradiation. *Radiation Oncol* 2015; 116:374-80.
 15. Oeck S, Szymonowicz K, Wiel G, Krysztofiak A, Lambert J, Koska B, et al. Relating linear energy transfer to the formation and resolution of DNA repair foci after irradiation with equal doses of X-ray photons, plateau, or Bragg-peak protons. *Int J Mol Sci* 2018; 19.
 16. Shibata A, Regulation of repair pathway choice at two-ended DNA double-strand breaks. *Mutat Res* 2017; 803-805:51-55.
 17. Gerelchuluun A, Zhu J, Su F, Asaithamby A, Chen DJ, Tsuboi K, Homologous recombination pathway may play a major role in high-LET radiation-induced DNA double-strand break repair. *J Radiat Res* 2014; 55:i83-i84.
 18. Hill MA, Herdman MT, Stevens DL, Jones NJ, Thacker J, Goodhead DT, Relative sensitivities of repair-deficient mammalian cells for clonogenic survival after alpha-particle irradiation. *Radiat Res* 2004; 162:667-76.
 19. Chaudhary P, Marshall TI, Currell FJ, Kacperek A, Schettino G, Prise KM, Variations in the processing of DNA double-strand breaks along 60-MeV therapeutic proton beams. *Int J Radiat Oncol Biol Phys* 2016; 95:86-94.
 20. Blackford AN, Jackson SP, ATM, ATR, and DNA-PK: The trinity at the heart of the DNA damage response. *Mol Cell* 2017; 66:801-17.
 21. Mansour WY, Rhein T, Dahm-Daphi J, The alternative end-joining pathway for repair of DNA double-strand breaks requires PARP1 but is not dependent upon microhomologies. *Nucleic Acids Res* 2010; 38:6065-77.
 22. Lourenco LM, Jiang Y, Drobnitzky N, Green M, Cahill F, Patel A, et al. PARP inhibition combined with thoracic irradiation exacerbates esophageal and skin toxicity in C57BL6 Mice. *Int J Radiat Oncol Biol Phys* 2018; 100:767-75.
 23. Jagsi R, Griffith KA, Bellon JR, Woodward WA, Horton JK, Ho A, et al. Concurrent veliparib with chest wall and nodal radiotherapy in patients with inflammatory or locoregionally recurrent breast cancer: The TBCRC 024 Phase I multicenter study. *J Clin Oncol* 2018; 36:1317-22.
 24. Loap P, Loirat D, Berger F, Cao K, Ricci F, Jochem A, et al. Combination of Olaparib with radiotherapy for triple-negative breast cancers: One-year toxicity report of the RADIOPARP Phase I trial. *International J Can* 2021; 149:1828-32.
 25. Bright SJ, Flint DB, Chakraborty S, McFadden CH, Yoon DS, Bronk L, et al. Nonhomologous end joining is more important than proton linear energy transfer in dictating cell death. *Int J Radiat Oncol Biol Phys* 2019; 105:1119-25.
 26. Titt U, Sahoo N, Ding X, Zheng Y, Newhauser WD, Zhu XR, et al. Assessment of the accuracy of an MCNPX-based Monte Carlo simulation model for predicting three-dimensional absorbed dose distributions. *Phys Med Biol* 2008; 53:4455-70.
 27. Flint DB, Bright SJ, McFadden CH, Konishi T, Ohsawa D, Turner B, et al. Cell lines of the same anatomic site and histologic type show large variability in intrinsic radiosensitivity and relative biological effectiveness to protons and carbon ions. *Med Phys* 2021; 48:3243-61.
 28. Kellerer AM, Hug O, Theory of dose-effect relations. In: Bauchinger M, Cronkite EP, Fliedner TM, Fritz-Niggli FH, Hug O, Kellerer AM, et al. editors. *Strahlenbiologie / Radiation Biology: Teil 3 / Part 3*. Place Springer Berlin Heidelberg: Springer Berlin Heidelberg; 1972.
 29. Kellerer AM, Hall EJ, Rossi HH, Teedla P, RBE as a function of neutron energy. II. Statistical analysis. *Radiat Res* 1976; 65:172-86.
 30. Fertil B, Dertinger H, Courdi A, Malaise EP, Mean inactivation dose: a useful concept for intercomparison of human cell survival curves. *Radiat Res* 1984; 99:73-84.
 31. ICRU, Quantitative Concepts and Dosimetry in Radiobiology. United States: International Commission on Radiation Units and Measurements, Washington, DC; 1979.
 32. Garcia-Barros M, Paris F, Cordon-Cardo C, Lyden D, Rafii S, Haimovitz-Friedman A, et al. Tumor response to radiotherapy regulated by endothelial cell apoptosis. *Science* 2003; 300:1155-9.
 33. Ciszewski WM, Tavecchio M, Dastych J, Curtin NJ, DNA-PK inhibition by NU7441 sensitizes breast cancer cells to ionizing radiation and doxorubicin. *Breast Can Res Treat* 2014; 143:47-55.
 34. Yu L, Shang Z-F, Hsu F-M, Zhang Z, Tumati V, Lin Y-F, et al. NSCLC cells demonstrate differential mode of cell death in response to the combined treatment of radiation and a DNA-PKs inhibitor. *Oncotarget* 2015; 6.
 35. Dong J, Ren Y, Zhang T, Wang Z, Ling CC, Li GC, et al. Inactivation of DNA-PK by knockdown DNA-PKs or NU7441 impairs non-homologous end-joining of radiation-induced double strand break repair. *Oncol Rep* 2018; 39:912-20.
 36. Sunada S, Kanai H, Lee Y, Yasuda T, Hirakawa H, Liu C, et al. Nontoxic concentration of DNA-PK inhibitor NU7441 radiosensitizes lung tumor cells with little effect on double strand break repair. *Cancer Sci* 2016; 107:1250-5.
 37. Fok JHL, Ramos-Montoya A, Vazquez-Chantada M, Wijnhoven PWG, Follia V, James N, et al. AZD7648 is a potent and selective DNA-PK inhibitor that enhances radiation, chemotherapy and olaparib activity. *Nat Commun* 2019; 10:5065.
 38. Zenke FT, Zimmermann A, Sirrenberg C, Dahmen H, Kirkin V, Pehl U, et al. Pharmacologic inhibitor of DNA-PK, M3814, potentiates radiotherapy and regresses human tumors in mouse models. *Mol Can Therap* 2020; 19:1091-101.

39. Willoughby CE, Jiang Y, Thomas HD, Willmore E, Kyle S, Wittner A, et al. Selective DNA-PKcs inhibition extends the therapeutic index of localized radiotherapy and chemotherapy. *J Clin Invest* 2020; 130:258-71.
40. Hammond EM, Muschel RJ, Radiation and ATM inhibition: the heart of the matter. *J Clin Invest* 2014; 124:3289-91.
41. Kim N, Kim SH, Kang S-G, Moon JH, Cho J, Suh C-O, et al. ATM mutations improve radio-sensitivity in wild-type isocitrate dehydrogenase-associated high-grade glioma: retrospective analysis using next-generation sequencing data. *Radiat Oncol* 2020; 15:184.
42. Worgul BV, Smilenov L, Brenner DJ, Junk A, Zhou W, Hall EJ, Atm heterozygous mice are more sensitive to radiation-induced cataracts than are their wild-type counterparts. *Proc Natl Acad Sci U S A* 2002; 99:9836-39.
43. Durant ST, Zheng L, Wang Y, Chen K, Zhang L, Zhang T, et al. The brain-penetrant clinical ATM inhibitor AZD1390 radiosensitizes and improves survival of preclinical brain tumor models. *Sci Adv* 2018; 4:eaat1719.
44. Riches LC, Trinidad AG, Hughes G, Jones GN, Hughes AM, Thomason AG, et al. Pharmacology of the ATM inhibitor AZD0156: Potentiation of irradiation and Olaparib responses preclinically. *Mol Can Therap* 2020; 19:13-25.
45. Tang S, Li Z, Yang L, Shen L, Wang Y, A potential new role of ATM inhibitor in radiotherapy: suppressing ionizing radiation-activated EGFR. *Int J Radiat Biol* 2020; 96:461-68.
46. Hanna C, Dunne VL, Walker SM, Butterworth KT, McCabe N, Waugh DJJ, et al. ATM kinase inhibition preferentially sensitises PTEN-deficient prostate tumour cells to ionising radiation. *Cancers (Basel)* 2020; 13.
47. Mladenov E, Fan X, Dueva R, Soni A, Iliakis G, Radiation-dose-dependent functional synergisms between ATM, ATR and DNA-PKcs in checkpoint control and resection in G2-phase. *Sci Rep* 2019; 9:8255.
48. Sundar R, Brown J, Ingles Russo A, Yap TA, Targeting ATR in cancer medicine. *Curr Probl Cancer* 2017; 41:302-15.
49. Dillon MT, Boylan Z, Smith D, Guevara J, Mohammed K, Peckitt C, et al. PATRIOT: A phase I study to assess the tolerability, safety and biological effects of a specific ataxia telangiectasia and Rad3-related (ATR) inhibitor (AZD6738) as a single agent and in combination with palliative radiation therapy in patients with solid tumours. *Clin Transl Radiat Oncol* 2018; 12:16-20.
50. Dillon MT, Barker HE, Pedersen M, Hafsi H, Bhide SA, Newbold KL, et al. Radiosensitization by the ATR inhibitor AZD6738 through generation of acentric micronuclei. *Mol Can Therap* 2017; 16:25.
51. Mladenova V, Mladenov E, Scholz M, Stuschke M, Iliakis G, Strong Shift to ATR-dependent regulation of the G(2)-checkpoint after exposure to high-LET radiation. *Life (Basel)* 2021; 11.
52. Sheng H, Huang Y, Xiao Y, Zhu Z, Shen M, Zhou P, et al. ATR inhibitor AZD6738 enhances the antitumor activity of radiotherapy and immune checkpoint inhibitors by potentiating the tumor immune microenvironment in hepatocellular carcinoma. *J Immunother Cancer* 2020; 8:e000340.
53. Vendetti FP, Karukonda P, Clump DA, Teo T, Lalonde R, Nugent K, et al. ATR kinase inhibitor AZD6738 potentiates CD8+ T cell-dependent antitumor activity following radiation. *J Clin Invest* 2018; 128:3926-40.
54. Szymonowicz K, Krysztofiak A, Linden JV, Kern A, Deycmar S, Oeck S, et al. Proton irradiation increases the necessity for homologous recombination repair along with the indispensability of non-homologous end joining. *Cells* 2020; 9.
55. Held KD, Kawamura H, Kaminuma T, Paz AE, Yoshida Y, Liu Q, et al. Effects of charged particles on human tumor cells. *Front Oncol* 2016; 6:23.
56. Vitti ET, Kacperek A, Parsons JL, Targeting DNA double-strand break repair enhances radiosensitivity of HPV-positive and HPV-negative head and neck squamous cell carcinoma to photons and protons. *Cancers (Basel)* 2020; 12.
57. Mladenova V, Mladenov E, Stuschke M, Iliakis G, DNA damage clustering after ionizing radiation and consequences in the processing of chromatin breaks. *Molecules* 2022; 27.
58. Lesueur P, Chevalier F, El-Habr EA, Junier MP, Chneiweiss H, Castera L, et al. Radiosensitization effect of talazoparib, a parp inhibitor, on glioblastoma stem cells exposed to low and high linear energy transfer radiation. *Sci Rep* 2018; 8:3664.
59. Senra JM, Telfer BA, Cherry KE, McCrudden CM, Hirst DG, O'Connor MJ, et al. Inhibition of PARP-1 by olaparib (AZD2281) increases the radiosensitivity of a lung tumor xenograft. *Mol Cancer Ther* 2011; 10:1949-58.
60. Wang L, Cao J, Wang X, Lin E, Wang Z, Li Y, et al. Proton and photon radiosensitization effects of niraparib, a PARP-1/-2 inhibitor, on human head and neck cancer cells. *Head & Neck* 2020; 42:2244-56.
61. Michmerhuizen AR, Pesch AM, Moubadder L, Chandler BC, Wilder-Romans K, Cameron M, et al. PARP1 inhibition radiosensitizes models of inflammatory breast cancer to ionizing radiation. *Mol Cancer Ther* 2019; 18:2063-73.
62. Fisher AE, Hochegger H, Takeda S, Caldecott KW, Poly(ADP-ribose) polymerase 1 accelerates single-strand break repair in concert with poly(ADP-ribose) glycohydrolase. *Mol Cell Biol* 2007; 27, 5597-605.
63. Robert I, Dantzer F, Reina-San-Martin B, Parp1 facilitates alternative NHEJ, whereas Parp2 suppresses IgH/c-myc translocations during immunoglobulin class switch recombination. *J Exp Med* 2009; 206:1047-56.
64. Iliakis G, Mladenov E, Mladenova V, Necessities in the processing of DNA double strand breaks and their effects on genomic instability and cancer. *Cancers (Basel)* 2019; 11.
65. Kim C, Wang XD, Yu Y, PARP1 inhibitors trigger innate immunity via PARP1 trapping-induced DNA damage response. *Elife* 2020; 9.
66. Michelena J, Lezaja A, Teloni F, Schmid T, Imhof R, Altmeyer M, Analysis of PARP inhibitor toxicity by multidimensional fluorescence microscopy reveals mechanisms of sensitivity and resistance. *Nat Commun* 2018; 9:2678.
67. Ma H, Takahashi A, Yoshida Y, Adachi A, Kanai T, Ohno T, et al. Combining carbon ion irradiation and non-homologous end-joining repair inhibitor NU7026 efficiently kills cancer cells. *Radiat Oncol* 2015; 10:225.
68. Du L-Q, Wang Y, Wang H, Cao J, Liu Q, Fan F-Y, Knockdown of Rad51 expression induces radiation- and chemo-sensitivity in osteosarcoma cells. *Med Oncol* 2011; 28:1481-87.
69. Gerelchuluun A, Manabe E, Ishikawa T, Sun L, Itoh K, Sakae T, et al. The major DNA repair pathway after both proton and carbon-ion radiation is NHEJ, but the HR pathway is more relevant in carbon ions. *Radiat Res* 2015; 183:345-56.